

Alma Mater Studiorum Università di Bologna  
Archivio istituzionale della ricerca

Highly Stereoregular 1,3-Butadiene and Isoprene Polymers through Monoalkyl- N-Aryl-Substituted Iminopyridine Iron Complex-Based Catalysts: Synthesis and Characterization

This is the final peer-reviewed author's accepted manuscript (postprint) of the following publication:

*Published Version:*

Ricci G., Leone G., Zanchin G., Palucci B., Boccia A.C., Sommazzi A., et al. (2021). Highly Stereoregular 1,3-Butadiene and Isoprene Polymers through Monoalkyl- N-Aryl-Substituted Iminopyridine Iron Complex-Based Catalysts: Synthesis and Characterization. *MACROMOLECULES*, 54(21), 9947-9959 [10.1021/acs.macromol.1c01291].

*Availability:*

This version is available at: <https://hdl.handle.net/11585/851695> since: 2023-06-09

*Published:*

DOI: <http://doi.org/10.1021/acs.macromol.1c01291>

*Terms of use:*

Some rights reserved. The terms and conditions for the reuse of this version of the manuscript are specified in the publishing policy. For all terms of use and more information see the publisher's website.

This item was downloaded from IRIS Università di Bologna (<https://cris.unibo.it/>).  
When citing, please refer to the published version.

(Article begins on next page)

This is the final peer-reviewed accepted manuscript of:

G. Ricci, G. Leone, G. Zanachin, B. Palucci, A. C. Boccia, A. Sommazzi, F. Masi, S. Zacchini, M. Guelfi, G. Pampaloni, "Highly Stereoregular 1,3-Butadiene and Isoprene Polymers through Monoalkyl-*N*-Aryl-Substituted Iminopyridine Iron Complex-Based Catalysts: Synthesis and Characterization", *Macromolecules*, **2021**, *54*, 9947-9959.

The final published version is available online at:

<https://doi.org/10.1021/acs.macromol.1c01291>

Terms of use:

Some rights reserved. The terms and conditions for the reuse of this version of the manuscript are specified in the publishing policy. For all terms of use and more information see the publisher's website.

# Highly Stereoregular 1,3-Butadiene and Isoprene Polymers through Monoalkyl-N-Aryl-Substituted Iminopyridine Iron Complex-Based Catalysts: Synthesis and Characterization

Giovanni Ricci<sup>a\*</sup>, Giuseppe Leone<sup>a</sup>, Giorgia Zanchin<sup>a</sup>, Antonella Caterina Boccia<sup>a</sup>, Anna Sommazzi<sup>b</sup>, Francesco Masi<sup>c</sup>, Stefano Zacchini<sup>d</sup>, Massimo Guelfi<sup>e</sup>, and Guido Pampaloni<sup>e</sup>.

<sup>a</sup>CNR-Istituto di Scienze e Tecnologie Chimiche "Giulio Natta" (SCITEC), via A. Corti 12, I-20133 Milano, Italy

<sup>b</sup>Versalis S.p.A. – Centro Ricerca Novara – Via G. Fauser 4, I-28100 Novara (NO), Italy

<sup>c</sup>Versalis S.p.A. - R&D Partner Catalysis – Piazza Boldrini 1, I-20097 San Donato Milanese (MI), Italy

<sup>d</sup>Università di Bologna, Dipartimento di Chimica Industriale "Toso Montanari", Viale Risorgimento 4, I-40136 Bologna, Italy

<sup>e</sup>Università di Pisa, Dipartimento di Chimica e Chimica Industriale, Via Moruzzi 13, I-56124 Pisa, Italy

**ABSTRACT:** A predominantly alternating *cis*-1,4-*alt*-3,4 polyisoprene, analogous to that previously obtained with the system  $\text{CoCl}_2(\text{PRPh}_2)_2$ -MAO (R = methyl, ethyl, *normal*-propyl, *iso*-propyl, cyclohexyl), was synthesized by polymerizing isoprene with iron catalysts obtained by combining pyridyl-imino complexes with methylaluminoxane (MAO). A complete NMR, thermal and rheological characterization of this novel polydiene having such an unusual structure was performed, which showed for this polymer a behavior quite similar to that of synthetic *cis*-1,4 polyisoprene.

## 1. Introduction

The research activity in the field of stereospecific polymerization of 1,3-dienes has focused in recent years on the study of catalytic systems based on organometallic complexes with various types of organic ligands having of N, O and P atoms as donor atoms[1].

The interest in these organometallic complexes having a well-defined structure is due to the fact that the ligand nature may play a fundamental role in determining the polymerization regio- and stereoselectivity[2], in controlling the polymer molecular weight and the molecular weight distribution, and in providing living features to the catalysts themselves[3].

Most of the work carried out concerned in particular cobalt-based catalysts [4] and to a lesser extent chromium [5], vanadium [6], titanium [7] and zirconium [8] based systems; in recent years, however, there has been a considerable rediscovery of iron-based systems, which have proved extremely active, selective, in some cases with living characteristics, and capable of polymerizing different types of conjugated dienes (*e.g.*, butadiene, isoprene, 2,3-dimethyl-1,3-butadiene, 3-methyl-1,3-pentadiene) providing stereoregular polymers of different structure from the different monomers. This last aspect specifically allowed us to improve and confirm our knowledge on the conjugated dienes polymerization mechanism [3].

Before the 2000s only a few papers were reported in the literature concerning the homo- and copolymerization of butadiene and isoprene with iron-based catalysts [9]. The interest in iron-based catalysts has subsequently increased considerably, also thanks to the great availability and cost-effectiveness of this metal, and to its sustainability and low environmental impact, if we consider its very low toxicity level if compared for example with that of systems based on chromium, nickel and cobalt.

Extremely active catalysts were first obtained by combining iron complexes with aromatic bidentate amines (*e.g.*, bipyridine or phenantroline) with  $AlR_3$  or MAO [10]; these systems gave highly stereoregular polydienes, in some cases never reported before (*e.g.*, syndiotactic 3,4 polyisoprene; syndiotactic (E)-1,2 poly(3-methyl-1,3-pentadiene) (Figure 1) [11].

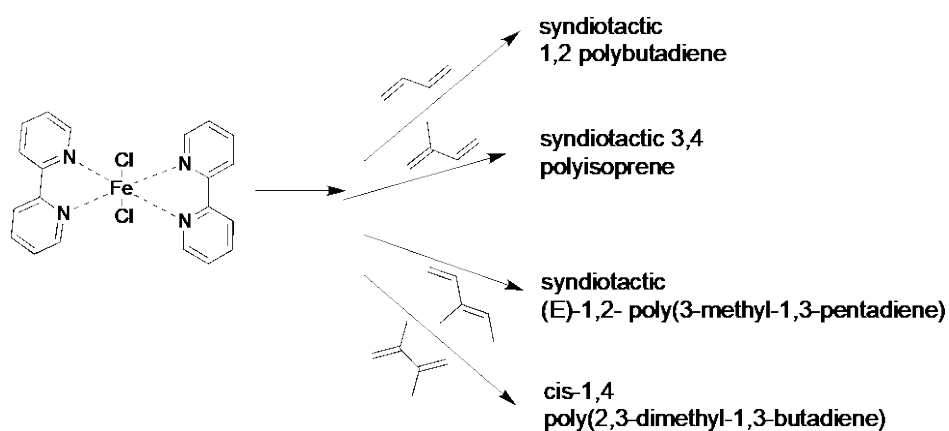


Figure 1.

Less active and selective catalysts, giving polyisoprenes with a mixed 1,2/3,4 structure and polybutadienes with predominantly *trans*-1,4 or mixed *cis/trans*/1,2 structures were obtained with iron complexes having chelating N,N,N-donor ligands (Figure 2) [12].

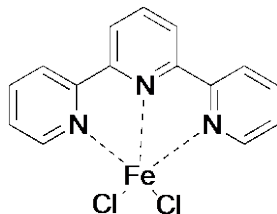
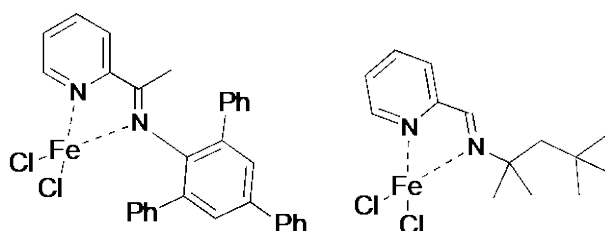


Figure 2.

An interesting class of iron systems, based on iminopyridine complexes, was introduced by Tobias Ritter et al in 2012[13]. Using two different types of iminopyridine complexes (Figure 3), in combination with an alkylating reagent (trialkylaluminum) and a dealkylating reagent (PheC+B(C6F5)4-, trityl BARF), for the polymerization of isoprene, he found that the imine moiety of the

iminopyridine ligand was able to control the selectivity of the providing *cis*-1,4 or *trans*-1,4 polyisoprenes depending on the nature of the ligand.



ligand was able to control monomer insertion, providing *cis*-1,4 or *trans*-1,4 polyisoprenes depending on the nature of the ligand.

Figure 3.

Further work on the polymerization of isoprene with catalysts based on alkyl- and aryl-substituted iminopyridine Fe(II) complexes was carried out by Changle Chen [14] and Marc Visseaux [15].

Specifically, by using di- and tri-substituted aryl iminopyridine Fe(II) complexes (Figure 4), Chen obtained predominantly *cis*-1,4 polyisoprenes with a 3,4 content up to 34%;

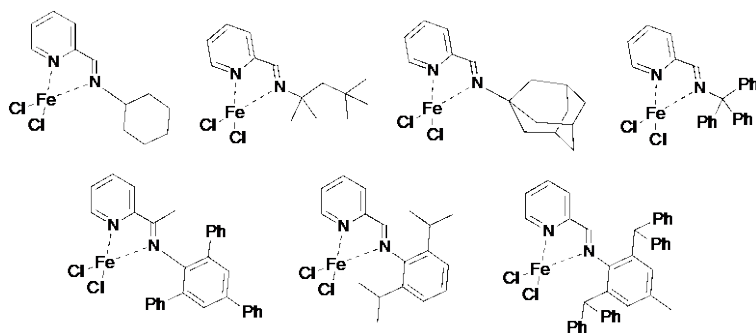


Figure 4.

by using di-substituted aryl iminopyridine Fe(II) complexes Visseaux obtained essentially 1,4 polyisoprenes (80-90%) having a predominantly *cis* or *trans* structure depending on the ligand nature, while mixed *cis*-1,4/3,4 polyisoprenes were obtained by using catalysts based on F-aryl substituted iminopyridine Fe(II) complexes (Figure 5).

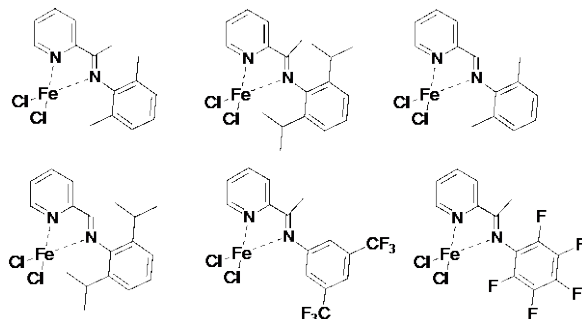


Figure 5

We also studied the polymerization of isoprene with catalysts based on substituted aryl iminopyridine iron complexes[16], and in particular, in case of mono-substituted aryl iminopyridine iron complexes (Figure 6), we were able to obtain a predominantly alternating *cis*-1,4-*alt*-3,4 polyisoprene, analogous to that previously obtained with the system  $\text{CoCl}_2(\text{PRPh}_2)_2\text{-MAO}$  (R = methyl, ethyl, *normal*-propyl, *iso*-propyl, cyclohexyl)[17]. A complete NMR and thermal characterization of this novel polydiene having such an unusual structure is reported.

## 2. Results and Discussion

### 2.1. Synthesis and characterization of ligands and complexes.

$\alpha$ -Anilinopyridine (L1-L3, Figure 6) were prepared via condensation with equimolar amine and 2-acetyl-pyridine or 2-pyridine-carboxyldehyde followed by reduction of the iminopyridine by sodium borohydride ( $\text{NaBH}_4$ ) as described in the literature[18].

(ANNA, credo che quei riferimenti coprano tutte le sintesi)

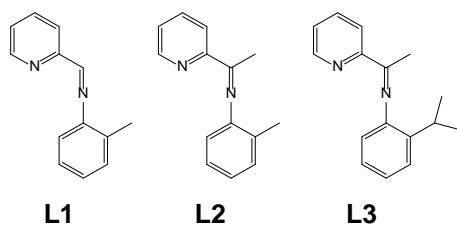


Figure 6.

The reactions of L1-L3 with iron chlorides (molar ratio = 1) are strongly dependent on the oxidation state of the metal.

The reactions with iron dichloride to give pure **Fe2L1-Fe2L3** (Figure 7), require heating at the reflux temperature of the mixture to microcrystalline solids stable in air for short period of times but to be stored under inert atmosphere. On the other hand, the reactions of **L1-L3** with  $\text{FeCl}_3$  are more complicated because biphasic liquid systems are generally obtained when using aromatic hydrocarbons (they are very slow in aliphatic hydrocarbons). Solid compounds can be obtained after prolonged drying of the oily residue in vacuo at room temperature and several washings with heptane. Compounds **Fe3L2-Fe3L3** (Figure 7) are moisture sensitive orange to brown microcrystalline solids. Products were characterized by analytical and infrared data. The main feature of the infrared spectra is the ca.  $20\text{ cm}^{-1}$  shift of the  $\text{C}=\text{N}$  absorption of the pyridylimino ligand towards lower wavenumbers due to the complexation, the shift being very similar for Fe(II) or Fe(III) derivatives.

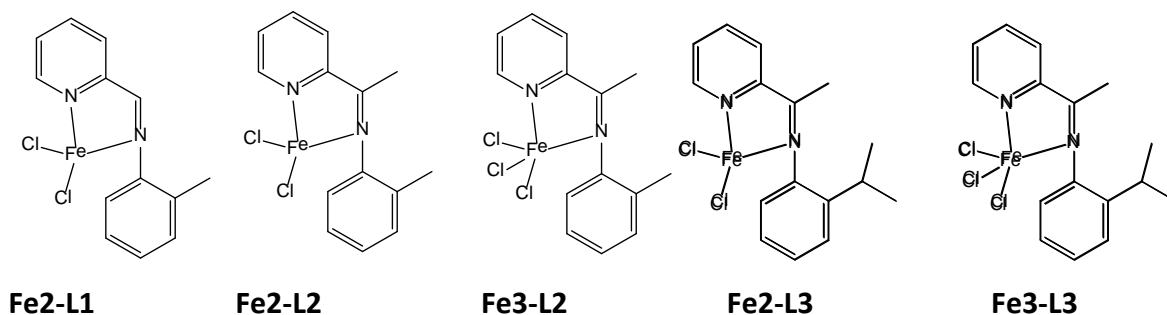


Figure 7.

The iron(II) adducts are soluble in polar solvents such as acetonitrile, have a limited solubility in aromatics and are substantially insoluble in saturated hydrocarbons. They react with protic solvents such as methanol or water with ligand disproportionation (vide infra).

Compound **Fe2-L3** has been recrystallized from  $\text{CH}_2\text{Cl}_2$  / heptane mixture and it has been characterized by X-ray diffraction methods. A view of the molecule is reported in Figure 8; table 1 lists a selection of bond distances and angles.

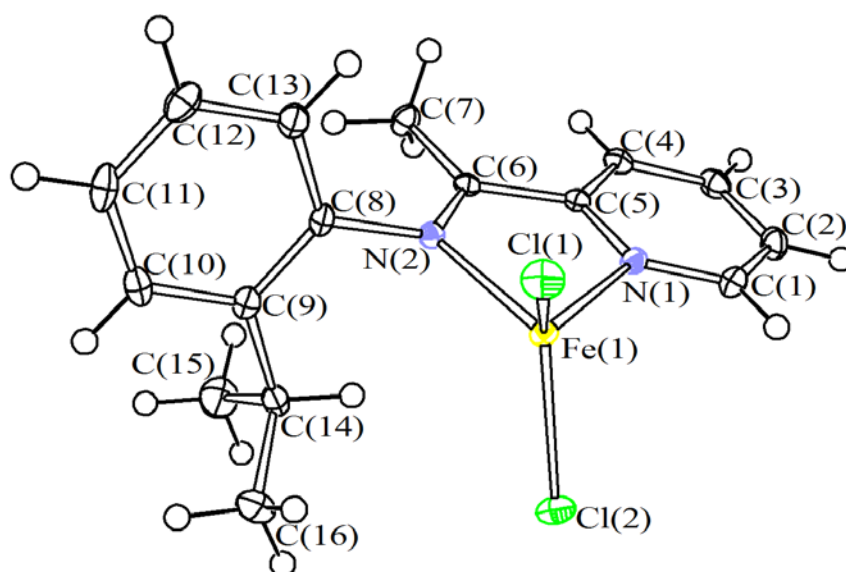


Figure 8. Molecular structure of **Fe2-L3**, with key atoms labeled. Displacement ellipsoids are at the 50% probability level.

Table1. Selection of bond distances (Å) and angles (gradi) for **Fe2-L3**.

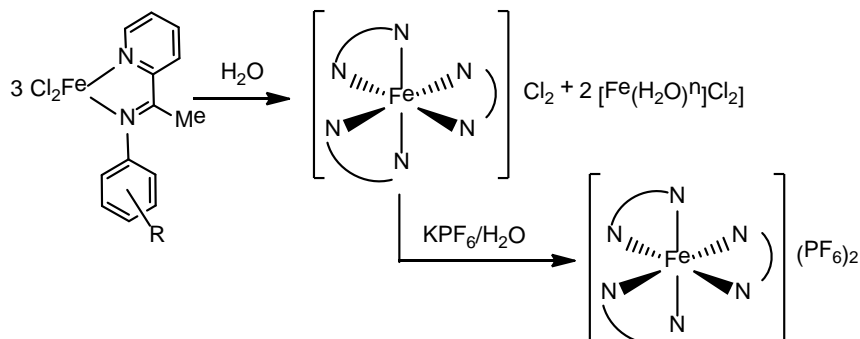
Fe(1)-Cl(1)	2.2331(5)	Fe(1)-Cl(2)	2.2371(5)
Fe(1)-N(1)	2.1098(16)	Fe(1)-N(2)	2.0938(15)
N(1)-C(5)	1.353(2)	N(2)-C(6)	1.284(2)
C(5)-C(6)	1.489(2)	N(2)-C(8)	1.437(2)
Cl(1)-Fe(1)-Cl(2)	119.60(2)	N(1)-Fe(1)-N(2)	77.16(6)
Fe(1)-N(1)-C(5)	114.54(12)	N(1)-C(5)-C(6)	114.97(16)
C(5)-C(6)-N(2)	115.80(16)	C(6)-N(2)-Fe(1)	117.39(12)

The solid-state structure shows the iron centre coordinated to two chlorides and two nitrogen atoms of the pyridylimino ligand. The coordination around iron is distorted tetrahedral, a coordination mode quite rare for adducts of  $\text{FeCl}_2$  with bidentate nitrogen ligands[19]. It is interesting to note that dinuclear structures (from X-ray determination) with pentacoordinated iron (distorted trigonal pyramidal coordination) have been described for strictly related complexes.[20]

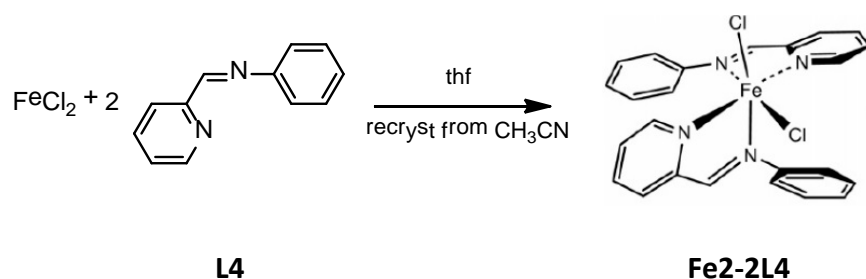
As 2,2'-dipyridyl and the 9,10-phenanthroline adducts of general formula  $\text{FeX}_2(\text{NN})_n$  ( $n = 1,2$ ) [21], **Fe2-L2** and **Fe2-L3** undergo disproportionation in water, vide infra, (Scheme 2) affording



tris(iminopyridyl) cations which can be isolated in high yields as the hexafluorophosphate by addition of  $\text{KPF}_6$ .



Some years ago, it was reported [22] that the reaction of  $\text{FeCl}_2$  with two equivalents of **L4** in thf followed by recrystallization from acetonitrile affords the bis-adduct **Fe2-L4** (Scheme 1).



Scheme 1

Being interested also to these compounds, we have found that the reaction between  $\text{FeCl}_2$  (either as thf adduct,  $\text{FeCl}_2(\text{thf})_{1,5}$ , or tetrahydrate,  $\text{FeCl}_2(\text{H}_2\text{O})_4$ ), affords different products according to the nature of the L/M molar ratio and of the medium. Table 2 reports the results obtained.

Table 2. Reactions of  $\text{FeCl}_2$  derivatives with **L4**

Run	Iron derivative, L5/Fe molar ratio	Medium	Temperature (°C) / time (h)	Product	Colour
1	$\text{FeCl}_2(\text{H}_2\text{O})_4$ , 1:1	toluene	25 / 3	$\text{FeCl}_2\text{L4}$	pale blue
2	$\text{FeCl}_2(\text{H}_2\text{O})_4$ , 2:1	toluene	25 / 3	$\text{FeCl}_2\text{L4}$	pale blue
3	$\text{FeCl}_2(\text{thf})_{1,5}$ , 1:1	thf	25 / 12	$\text{FeCl}_2\text{L4}$	pale violet
4	$\text{FeCl}_2(\text{thf})_{1,5}$ , 2:1	thf	80 / 3	$\text{FeCl}_2(\text{L4})_2$	pale blue
5	$\text{FeCl}_2(\text{thf})_{1,5}$ , 2:1	toluene	80 / 3	$\text{FeCl}_2\text{L4}$	pale blue

6	$\text{FeCl}_2(\text{H}_2\text{O})_4$ , 3:1	$\text{H}_2\text{O}$	25 / 3	$[\text{Fe}(\mathbf{L4})_3]\text{Cl}_2$	pale blue
---	---	----------------------	--------	---	-----------

By performing the reaction in thf, the bis adduct  $\text{FeCl}_2(\mathbf{L4})_2$  could be obtained (Item 4) which was identified by analytical data and X-ray diffraction methods as its  $\text{FeCl}_2(\mathbf{L4})_2 \cdot \text{MeOH}$  solvated crystal. The molecular structure of  $\text{FeCl}_2(\mathbf{L4})_2$  has been previously reported as its  $\text{FeCl}_2(\mathbf{L4})_2 \cdot \text{MeCN}$  solvated crystal [22], displaying almost identical bonding parameters and overall connectivity. For sake of completeness, the crystal data of the new solvate have been deposited within the Cambridge Crystallographic Data Center and a representation of the molecular structure of  $\text{FeCl}_2(\mathbf{L4})_2$  together with its most relevant bonding parameters are reported in the Supporting Information. (see Figure S1 and Table S1 ).

While attempting to prepare **Fe3-L3**, the oily residue obtained after evaporation of the volatiles was treated with methanol and the solution was kept at ca. 4 °C for some weeks. A small yield of orange crystals was obtained, which were identified as the hexanuclear  $\text{Fe}_6\text{Cl}_6(\mu_4\text{-O})(\mu_2\text{-OMe})_2\{[\text{N,N}(\text{C}_5\text{H}_5\text{N})\text{C}(\text{CH}_3)\text{N}(2\text{-}^i\text{Pr})\text{C}_6\text{H}_4]\}_2$ . The compound has been characterized by analytical data and by X-ray diffraction methods. A view of the structure is reported in Figure 9. Table 3 lists a selection of bond distances and angles.

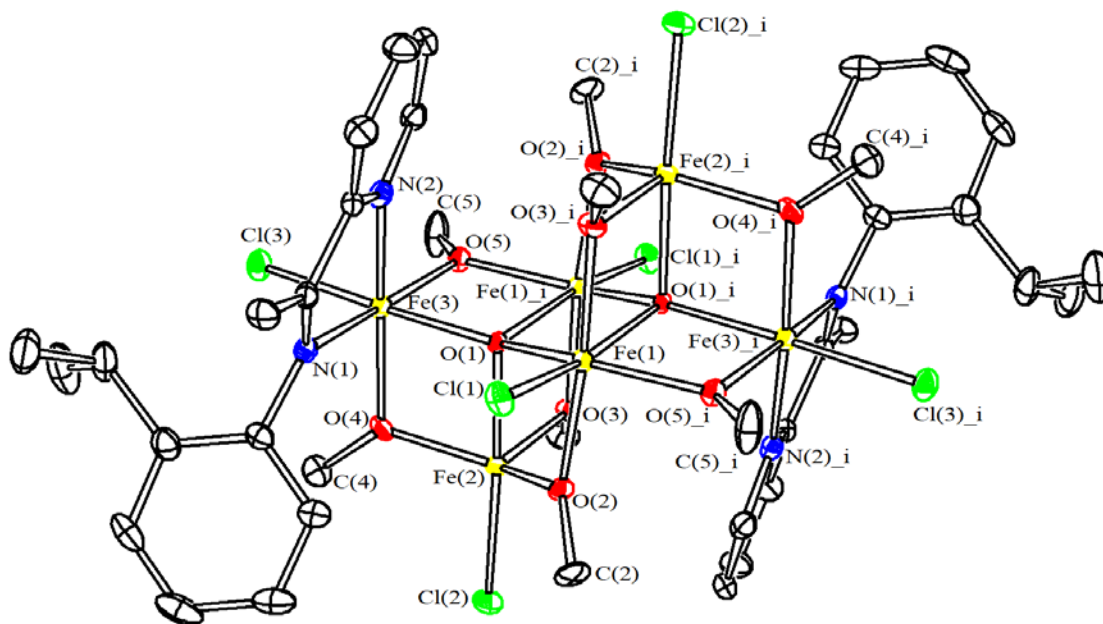


Figure 9. Molecular structure of  $\text{Fe}_6\text{Cl}_6(\mu_4\text{-O})(\mu_2\text{-OMe})_2\{[\text{N},\text{N}-(\text{C}_5\text{H}_5\text{N})\text{C}(\text{CH}_3)\text{N}(2\text{-}^i\text{Pr})\text{C}_6\text{H}_4]\}_2$  with key atoms labeled.

Displacement ellipsoids are at the 50% probability level. Symmetry transformations used to generate equivalent atoms:  $-x+1, -y+1, -z+1$ .

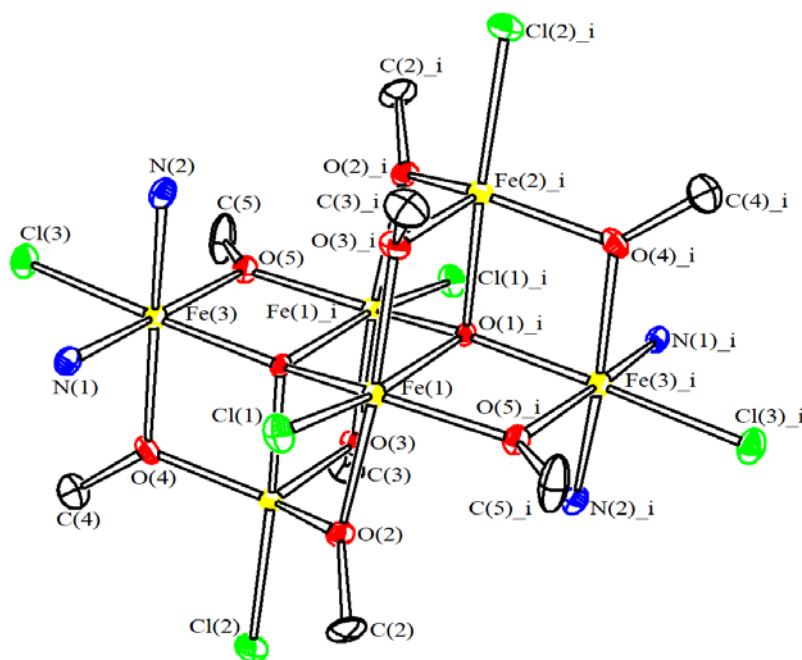
Table 4. Selection of bond distances (Å) and angles (deg) for  $\text{Fe}_6\text{Cl}_6(\mu_4\text{-O})(\mu_2\text{-OMe})_2\{[\text{N},\text{N}-(\text{C}_5\text{H}_5\text{N})\text{C}(\text{CH}_3)\text{N}(2\text{-}^i\text{Pr})\text{C}_6\text{H}_4]\}_2$ . Symmetry transformations used to generate equivalent atoms:  $-x+1, -y+1, -z+1$ .

Fe(1)—O(1)	1.959(3)	Fe(1)—O(5)_i	2.004(3)
Fe(1)—O(2)	2.062(3)	Fe(1)—O(3)_i	2.062(3)
Fe(1)—O(1)_i	2.121(3)	Fe(1)—Cl(1)	2.2859(14)
Fe(2)—O(3)	1.902(3)	Fe(2)—O(2)	1.915(3)
Fe(2)—O(4)	1.940(4)	Fe(2)—O(1)	2.082(3)
Fe(2)—Cl(2)	2.2647(15)	Fe(3)—O(1)	1.994(3)
Fe(3)—O(4)	1.995(4)	Fe(3)—O(5)	1.997(3)
Fe(3)—N(2)	2.122(4)	Fe(3)—N(1)	2.208(4)
Fe(3)—Cl(3)	2.2856(14)		
O(1)—Fe(1)—O(5)_i	147.13(14)	O(1)—Fe(1)—O(2)	77.32(13)
O(5)_i—Fe(1)—O(2)	91.02(14)	O(1)—Fe(1)—O(3)_i	98.23(14)
O(5)_i—Fe(1)—O(3)_i	94.31(14)	O(2)—Fe(1)—O(3)_i	174.66(14)
O(1)—Fe(1)—O(1)_i	77.86(14)	O(5)_i—Fe(1)—O(1)_i	75.20(13)
O(2)—Fe(1)—O(1)_i	103.56(13)	O(3)_i—Fe(1)—O(1)_i	78.12(13)
O(1)—Fe(1)—Cl(1)	108.32(10)	O(5)_i—Fe(1)—Cl(1)	102.01(10)
O(2)—Fe(1)—Cl(1)	89.09(10)	O(3)_i—Fe(1)—Cl(1)	89.54(10)
O(1)_i—Fe(1)—Cl(1)	167.01(10)	O(3)—Fe(2)—O(2)	109.79(15)
O(3)—Fe(2)—O(4)	106.25(15)	O(2)—Fe(2)—O(4)	134.39(15)
O(3)—Fe(2)—O(1)	82.71(14)	O(2)—Fe(2)—O(1)	77.77(14)
O(4)—Fe(2)—O(1)	80.09(14)	O(3)—Fe(2)—Cl(2)	104.87(11)
O(2)—Fe(2)—Cl(2)	97.90(11)	O(4)—Fe(2)—Cl(2)	98.92(11)
O(1)—Fe(2)—Cl(2)	172.27(11)	O(1)—Fe(3)—O(4)	80.97(14)
O(1)—Fe(3)—O(5)	78.26(14)	O(4)—Fe(3)—O(5)	98.54(15)
O(1)—Fe(3)—N(2)	89.46(15)	O(4)—Fe(3)—N(2)	159.99(16)
O(5)—Fe(3)—N(2)	96.63(16)	O(1)—Fe(3)—N(1)	93.46(14)
O(4)—Fe(3)—N(1)	88.79(15)	O(5)—Fe(3)—N(1)	167.85(15)
N(2)—Fe(3)—N(1)	74.20(16)	O(1)—Fe(3)—Cl(3)	173.05(11)
O(4)—Fe(3)—Cl(3)	97.86(11)	O(5)—Fe(3)—Cl(3)	95.20(11)
N(2)—Fe(3)—Cl(3)	93.67(12)	N(1)—Fe(3)—Cl(3)	93.36(11)

The structure of the molecule consists of two  $\text{Fe}_3$  units connected by quadruply bridged oxygen atoms and bridging methoxy groups. The core of iron atoms is made of two tetrahedra sharing a vertex, and the two  $\text{Fe}_3$  units are correlated by an inversion centre. Fe(1) displays a distorted octahedral coordination being bonded to one terminal chloride, three  $\mu\text{-OMe}$  and two  $\mu_4\text{-O}$  ligands (Figure 10). Also Fe(3) adopts a distorted octahedral coordination involving one terminal chloride, two  $\mu\text{-OMe}$  and one  $\mu_4\text{-O}$  ligands as well as two nitrogens of a bidentate imino ligand. Conversely, Fe(2) is pentacoordinated to one terminal chloride, three  $\mu\text{-OMe}$  and one  $\mu_4\text{-O}$  ligands. The overall geometry

around Fe(2) may be described as a trigonal bipyramid with the three  $\mu$ -OMe ligands in the equatorial plane.

Figure 10. View of the iron coordination within the internal core of  $\text{Fe}_6\text{Cl}_6(\mu_4\text{-O})(\mu_2\text{-OMe})_2\{[\text{N,N}-(\text{C}_5\text{H}_5\text{N})\text{C}(\text{CH}_3)\text{N}(2\text{-}^i\text{Pr})\text{C}_6\text{H}_4]\}_2$



Literature reports several examples of polynuclear iron(III) compounds containing oxides and methoxides as bridging ligands. Generally, they show high nuclearity and interesting magnetic properties [21, 23].

## 2.2. Polymerization of isoprene.

All the above reported iron complexes were used, in combination with methylaluminixane, for the polymerization of isoprene. The results obtained are shown in Table 4.

Table 4. Polymerization of isoprene with mono-alkyl substituted aryliminopyridine iron complexes based catalysts.<sup>a</sup>

exp	complex	$\mu\text{mol}$	Al/Fe (molar ratio)	T (min)	conv. (%)	<i>cis</i> -1,4 (%)	3,4 (%)	Tg (°C)	Mw g/mol	M <sub>w</sub> /M <sub>n</sub>
IP461		5	1000	3	100	57,9	42,1		1067000	3,9
IP462	<b>Fe2-L1</b>	10	100	3	100	57,9	42,1		409500	2,8
IP463		20	10	20	62	56,7	43,3		91900	1,8
ZG189	<b>Fe2-L2</b>	10	50	5	100	58,5	41,5	-29,7	260800	1,8
IP205/A	<b>Fe3-L2</b>	10	50	5	100	59,1	40,9	-29,3	369900	1,9
ZG188	<b>Fe2-L3</b>	10	50	10	100	59,3	40,7	-31,9	244700	2,0
IP206/A	<b>Fe3-L3</b>	10	50	5	100	57,7	42,3		355600	2,0

<sup>a</sup> Polymerization conditions: isoprene, 2 ml; solvent toluene, total volume, 16 ml; MAO; 22°C.

All the catalyst systems are extremely active since complete monomer conversions are reached in a few minutes; the catalyst activity seems to decrease with decreasing the MAO/Fe molar ratio, nevertheless it was found to be quite high also at very low molar ratio (about 10).

The polymer molecular weight was rather high, decreasing with decreasing the MAO/Fe molar ratio; the molecular weight distribution was found to be in general quite narrow, in agreement with a single site nature of the catalyst systems.

As regards the polymer microstructure, all the polyisoprenes synthesized exhibited a mixed *cis*-1,4/3,4 structure, being the *trans*-1,4 units almost negligible, independently on the catalyst structure (*i.e.*, type of ligand and iron oxidation state) and on the polymerization conditions (*i.e.*, MAO/Fe molar ratio).

The *cis*-1,4 and 3,4 units, however, are not randomly distributed along the polymer chain, but the polymer, as clearly indicated by the NMR analysis (<sup>1</sup>H, <sup>13</sup>C and 2D), exhibits a predominantly alternating *cis*-1,4-*alt*-3,4 structure, very similar to that of the polyisoprene previously synthesized with the systems CoCl<sub>2</sub>(PRPh<sub>2</sub>)<sub>2</sub>-MAO (R = methyl, ethyl, *normal*-propyl, *iso*-propyl or cyclohexyl). However, the two polymers have a substantial difference: the Co-polyisoprenes exhibit a perfectly alternating *cis*-1,4-*alt*-3,4 structure, while in the Fe-polyisoprenes some very short *cis*-4 unit sequences (three units) are detectable along the polymer chain. Such a difference, well pointed out by the NMR analysis, has a quite remarkable impact on the glass transition temperature of the two different polymers, around -15°C for the Co-polymer <sup>[17]</sup> and around -30 ° C in case of the Fe-polyisoprene.

### 2.3. Polymer characterization.

The FT-IR spectrum of the polymer of Table 1 run xxx is shown in Figure 8. Peaks at  $840\text{ cm}^{-1}$  and  $890\text{ cm}^{-1}$  are indicative of the presence of 1,4 and 3,4 units, respectively.

The amount of 1,4 and 3,4 units can be deduced by the  $^1\text{H}$  NMR spectrum (Figure 9).

The  $^{13}\text{C}$  NMR spectrum is instead shown in Figure 10; peaks corresponding to *trans*-1,4 units (.....ppm) are not detectable, confirming indeed the absence of such units.

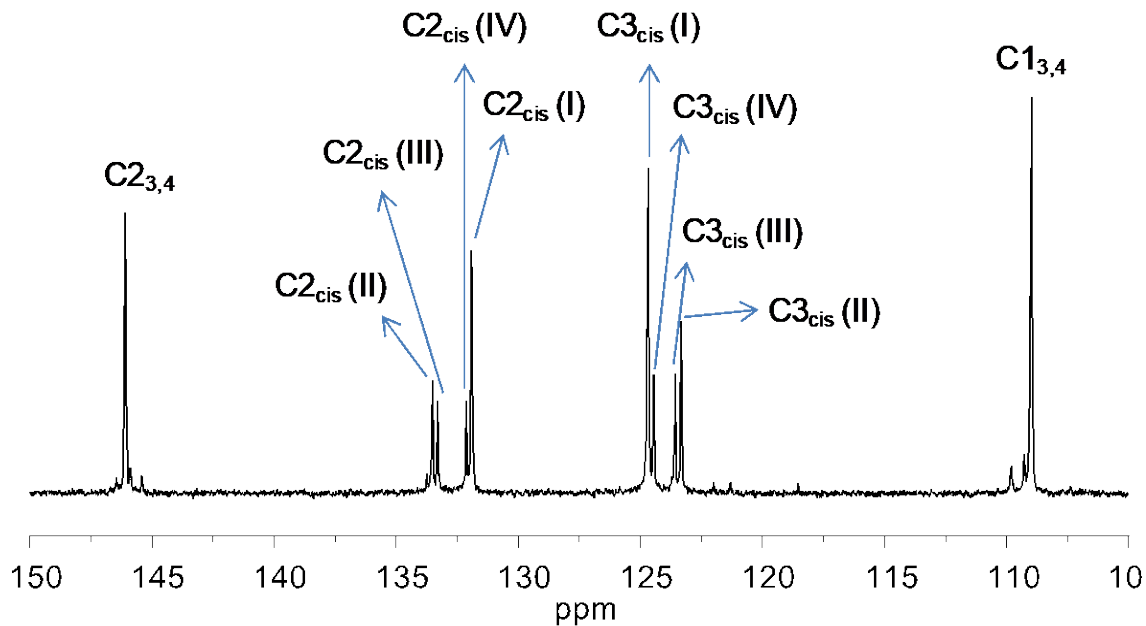


Figure 10.

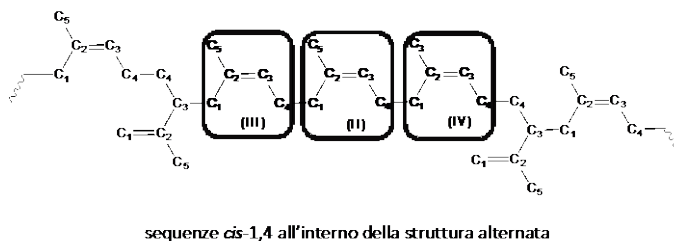
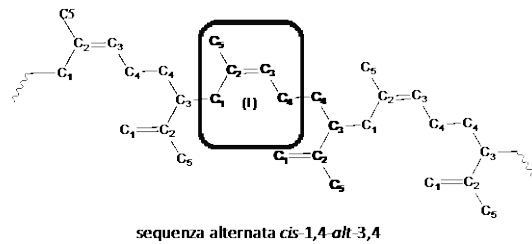
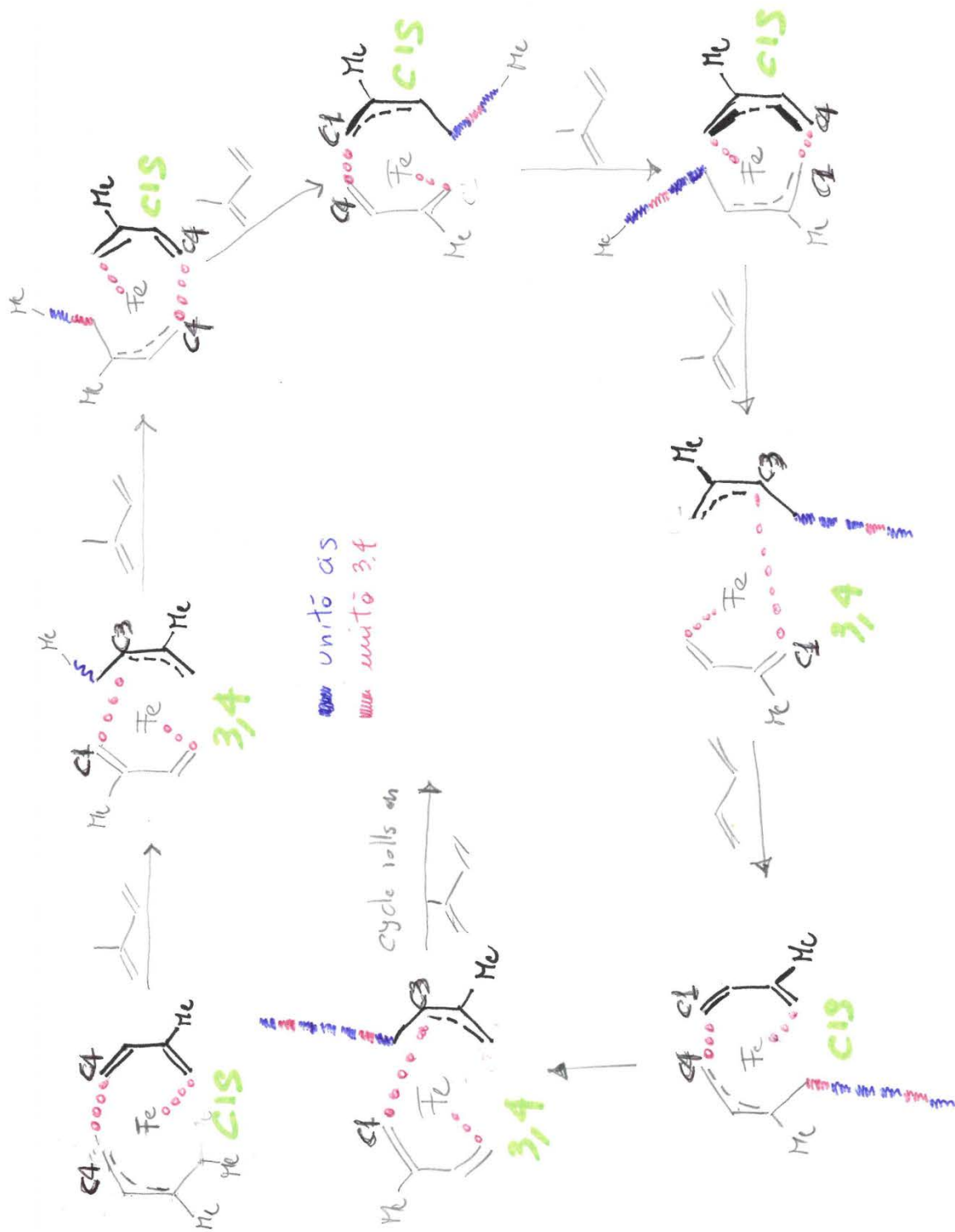


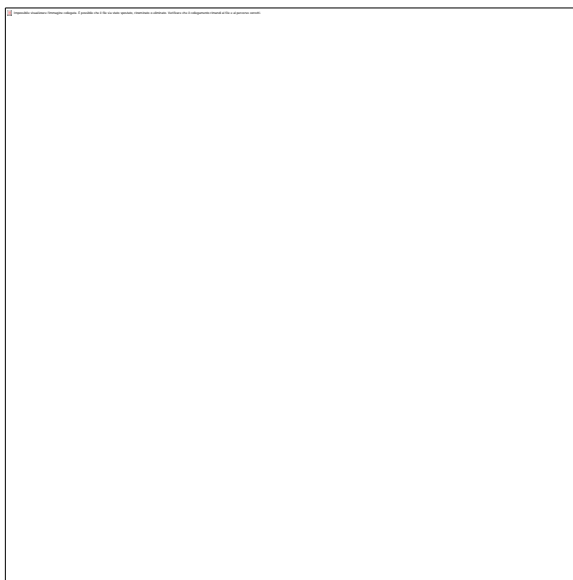
Figure 11.

As regards the formation of this somewhat unusual polymeric structure, a possible plausible





mechanism is shown in Figure 12:



.....  
.....  
.....

### 3. Conclusion

New iron pyridylimino derivatives have been prepared and characterized. The examples reported in the paper include iron(III) derivatives of general formula  $\text{FeCl}_3\text{L}$ , which can be isolated as solid compounds with some difficulty. They result quite moisture sensitive. In one case, partial hydrolysis in methanol afforded a hexanuclear iron(III) derivative containing oxo, methoxo and pyridylimino groups as ligands.

A novel polyisoprene, having a predominantly alternating *cis*-1,4-*alt*-3,4 structure but exhibiting some very short *cis*-1,4 units sequences along the polymer chain, was obtained with iminopyridine iron complexes based catalysts. The polymer has a transition glass temperature of about  $-30^\circ\text{C}$ , lower with respect to that of the perfectly alternating *cis*-1,4-*alt*-3,4 polyisoprenes synthesized with diphenylalkyl phosphines cobalt complexes based catalysts. The lower  $T_g$  is likely attributable to the presence of the *cis*-1,4 sequences; work is in progress with other iminopyridine iron complexes having different substitution on the phenyl ring in order to verify the possibility of lengthening the *cis*-1,4 sequences within the polymeric chain, thus bringing the properties of these new polyisoprenes closer to those of the natural rubber.

### 4. Experimental

**4.1. Materials.** Unless otherwise stated, manipulations of air- and/or moisture-sensitive materials were carried out under an inert atmosphere using a dual vacuum/nitrogen line and standard Schlenk-

line techniques. Nitrogen was purified by passage over columns of  $\text{CaCl}_2$ , molecular sieves and BTS catalysts or by passage over the columns Alphagaz Purifiers  $\text{O}_2$ -Free and  $\text{H}_2\text{O}$ -Free (Air Liquide). Thf (Aldrich,  $\geq 99.9\%$ ) was refluxed over Na/benzophenone for 8 h and then distilled. Toluene and heptane (Aldrich,  $>99.5\%$ ) were refluxed over Na for 8 h and then distilled and stored over molecular sieves. Isoprene (Fluka,  $\geq 99.5\%$ ) was refluxed over calcium hydride for 3 h, then distilled trap-to-trap and stored under dry nitrogen. Iron dichloride, iron trichloride and iron dichloride tetrahydrate were commercial products (Aldrich) used without purification. The thf adduct  $\text{FeCl}_2(\text{thf})_{1,5}$  was prepared according to literature [19c]. MAO (Aldrich, 10 wt% solution in toluene), tetrachloroethane- $\text{d}_2$  ( $\text{C}_2\text{D}_2\text{Cl}_4$ ) (Aldrich,  $>99.5\%$  atom D), 2-pyridinecarboxaldehyde (Aldrich), 2-acetylpyridine (Aldrich), 2-*iso*-propylaniline (Aldrich), 2-methylaniline (Aldrich), were used as received. 2-Methyl(pyridin-2-ylmethyl)aniline, **L1**, 2-Methyl(pyridin-2-ylethyl)aniline, **L2**, 2-isopropyl(pyridin-2-ylethyl)aniline, **L3**, were prepared according to the literature procedure [18].

Elemental Analysis were performed with a Perkin Elmer CHN Analyzer 2400 Series. The  $^1\text{H}$ - and  $^{13}\text{C}$ -NMR spectra were recorded using a nuclear magnetic resonance spectrometer mod. Bruker Avance 400, using deuterated tetrachloroethane ( $\text{C}_2\text{D}_2\text{Cl}_4$ ) at  $103^\circ\text{C}$ , and hexamethyldisiloxane (HDMS) as internal standard, or deuterated chloroform ( $\text{CDCl}_3$ ) or dichloromethane- $\text{d}_2$  ( $\text{CD}_2\text{Cl}_2$ ), at  $25^\circ\text{C}$ , and tetramethylsilane (TMS) as internal standard. Polymer solutions were used with concentrations equal to 10% in weight with respect to the total weight of the polymer solution. The microstructure of polymers [i.e. *cis*-1,4 unit content (%) and 3,4 unit content (%)] was determined through the analysis of the spectra based on literature [24].

The FTIR-ATR spectra of ligands and complexes were recorded using a Bruker IFS 48 or a Perkin Elmer Spectrum One spectrophotometers equipped with a Thermo Spectra-Tech horizontal ATR connection. The FT-IR spectra of the polymers were obtained from polymeric films on potassium bromide (KBr) tablets. Films were obtained through the evaporation of the solvent from a solution in hot 1,2-dichlorobenzene. The concentration of the polymeric solutions analyzed was equal to 10% in weight with respect to the total weight of the polymeric solution.

The determination of the molecular weight (MW) of the polymers was performed through GPC (Gel Permeation Chromatography) operating under the following conditions: Agilent 1100 pump; Agilent 1100 I.R. detector; PL Mixed-A columns; solvent/eluent: tetrahydrofuran (THF); flow rate: 1 ml/min; temperature:  $25^\circ\text{C}$ ; molecular mass calculation: Universal Calibration method. The weight-average

molecular weight ( $M_w$ ) and the Polydispersion Index (PDI) are reported, corresponding to the ratio  $M_w/M_n$  ( $M_n$  = number-average molecular weight).

Gas chromatography-mass spectrometry (GC-MS) was performed using a Thermo ISQ single quadrupole mass spectrometer. Samples of the ligands were dissolved in methylene chloride ( $\text{CH}_2\text{Cl}_2$ ) at a concentration of 0.1 mg/ml and were analyzed using said spectrometer operating under the following conditions: ionization method: electronic ionization (EI); GC ramp: 50°C for 2 minutes, heating at a speed of 10°C/min to 300°C; injector temperature: 300°C; injection volume: 1  $\mu\text{l}$ ; transfer line temperature: 280°C; temperature of the ionic source: 250°C; quadrupole scan parameters: 35 amu - 500 amu with scan time of 0.2 sec.

ANNA, GIOVANNI: controllate se quanto scritto sopra è corretto e non ci sono reagenti che non rientrano in questo lavoro. Ho infatti ripreso la PS dal lavoro sul titanio già pubblicato.

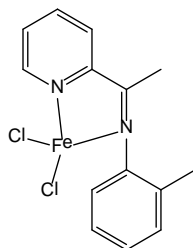
#### 4.2. Synthesis and characterization of ligands

ANNA, GIOVANNI: *Se è vero quanto scritto sopra, questo paragrafo si può togliere*

#### 4.3. Synthesis and characterization of complexes

##### 4.3.1. Iron(II) derivatives

Only the preparation of **Fe2-L2** is described in detail, the others being performed under similar experimental conditions.



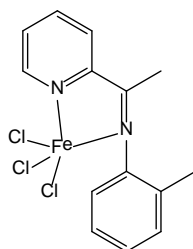
A solution of **L2** (527 mg; 2,51 mmol) in toluene (20 ml), was added of solid  $\text{FeCl}_2$  (319 mg; 2,51 mmol; molar ratio **L2**/Fe = 1). The mixture was stirred for 3h at ca 80°C. Volatiles were removed in vacuo at room temperature and the residue was washed with heptane (2 x 15 ml), dried in vacuo at room temperature affording 0.521 g (62 % yield) of **Fe2-L2** as blue microcrystalline solid. Anal. Found (Calcd. for  $\text{C}_{14}\text{H}_{14}\text{Cl}_2\text{FeN}_2$ ): C: 49,10% (49,89%), H: 4,38% (4,19%), N: 8,21% (8,31%), Cl: 21,42% (21,04%), Fe: 16,82% (16,57%). IR (solid state,  $\text{cm}^{-1}$ ):  $\nu = 3063\text{w}, 3012\text{w}, 2952\text{w}, 2916\text{w}, 1629\text{m}, 1593\text{s}, 1567\text{m-w}, 1483\text{s}, 1367\text{m-s}, 1315\text{m}, 1253\text{m}, 1217\text{m}, 800\text{vs}, 779\text{vs}, 754\text{vs}, 717\text{m}$ .

**Fe2-L1**.pale blue, from FeCl<sub>2</sub> (2.54 mmoli) and **L1**, molar ratio L1/Fe = 1. 78 % yield. Anal. Found (Calcd. for C<sub>13</sub>H<sub>12</sub>Cl<sub>2</sub>FeN<sub>2</sub>): C: 52,12% (48.34%), H: 4,65% (3.74%), N: 7,26% (8.67%), Cl: 19,02% (21.95%), Fe: 15,04% (17.29%). IR (solid state, cm<sup>-1</sup>): ν = 3071w, 3021w, 2963m, 1640m, 1595s, 1484m, 1363m, 1307m-w, 1210m, 1012m, 904m, 774vs, 768vs, 755vs.

**Fe2-L3**.pale blue, from FeCl<sub>2</sub> (2,27 mmoli) and **L3**, molar ratio **L3**/Fe = 1.80% yield. Anal. Found (Calcd. for C<sub>16</sub>H<sub>18</sub>Cl<sub>2</sub>FeN<sub>2</sub>): C: 52,12% (52,64%), H: 4,65% (4,96%), N: 7,26% (7,67%), Cl: 19,02% (19,42%), Fe: 15,04% (15,30%). IR (solid state, cm<sup>-1</sup>): ν = 3060w, 2961m, 2925w, 2866w, 1626m, 1593s, 1487m, 1444m, 1371m, 1318m, 1253m, 1255m-s, 1020m, 849m, 800vs, 790s, 772vs.

#### 4.3.2. Iron(III) derivatives

Only the preparation of **Fe3-L2** is described in detail, the others being performed under similar experimental conditions.



A solution of **L2** (293 mg; 1,39 mmol) in toluene (20 ml), was added of solid FeCl<sub>3</sub> (225 mg; 1,39 mmol; molar ratio **L2**/Fe = 1). The mixture was stirred for 3h at room temperature. Volatiles were removed in vacuo at room temperature and the residue was washed with heptane (2 x 15 ml), dried in vacuo at room temperature affording 0.396 g (76 % yield) of **Fe3-L2** as brown microcrystalline solid. Anal. Calcd. for C<sub>14</sub>H<sub>14</sub>Cl<sub>3</sub>FeN<sub>2</sub>): C: 45,00% (45,14%), H: 3,69% (3,79%), N: 7,69% (7,52%), Cl: 28,96% (28,55%), Fe: 15,09% (14,99%). ν = 3080w, 3023w, 2922w, 1625m, 1595s, 1486m, 1445m, 1372m, 1305m, 1259m, 1023m, 801m, 781vs, 743s, 716m, 651m.

**Fe3-L3**.red, from FeCl<sub>3</sub> (2,16 mmol) and **L3**, molar ratio **L3**/Fe = 1. 95% yield. Found (Calcd. for C<sub>16</sub>H<sub>18</sub>Cl<sub>3</sub>FeN<sub>2</sub>): C: 48,09% (47,97%), H: 4,71% (4,53%), N: 6,65% (6,99%), Cl: 25,96% (26,55%), Fe: 14,08% (13,94%). IR (solid state, cm<sup>-1</sup>): ν = 3067w, 3026w, 2966m, 2925w, 2869w, 1622m, 1595s, 1484m, 1444m, 1372m, 1319m, 1258m, 1023m, 801m, 777s, 756vs, 734sm, 696m.

#### 4.3.3. Synthesis of Fe<sub>6</sub>Cl<sub>6</sub>(μ<sub>4</sub>-O)(μ<sub>2</sub>-OMe)<sub>2</sub>{[N,N-(C<sub>5</sub>H<sub>5</sub>N)C(CH<sub>3</sub>)N(2-<sup>i</sup>Pr)C<sub>6</sub>H<sub>4</sub>]}<sub>2</sub>

A solution of **L3** (0.47 g; 1.97 mmol) in toluene (20 ml), was added of solid  $\text{FeCl}_3$  (0.32 mg; 1.97 mmol; molar ratio **L3**/Fe = 1). The mixture was stirred for 3h at room temperature. Volatiles were removed in vacuo at room temperature and the oily residue was dissolved in methanol (5 ml) and stored at ca. 4°C. After three weeks, red-orange crystals were present which were isolated, quickly dried in vacuo at room temperature, affording  $\text{Fe}_6\text{Cl}_6(\mu_4\text{-O})(\mu_2\text{-OMe})_2\{[\text{N,N}-(\text{C}_5\text{H}_5\text{N})\text{C}(\text{CH}_3)\text{N}(2\text{-}^i\text{Pr})\text{C}_6\text{H}_4]\}_2$  (12 mg, 3.4 % yield with respect to iron introduced). Found (Calcd. for  $\text{C}_{34}\text{H}_{42}\text{Cl}_6\text{Fe}_6\text{N}_4\text{O}_2$ ): C: 37.11% (37.58%), H: 4.09% (3.90%), N: 5.36% (5.16%), Cl: 19.05% (19.58%), Fe: 30.12% (30.84%).

#### 4.3.4. Treatment of **Fe2-Ln** ( $n = 2,3$ ) with water. Synthesis of $\text{Fe}(\text{Ln})_3](\text{PF}_6)_2$

Only the preparation of  $\text{Fe}(\text{L3})_3](\text{PF}_6)_2$  is described in detail, the other being performed under similar experimental conditions.

Solid **Fe2-L3** (0.23 g; 0.63 mmol) was added to water (10 ml) obtaining a magenta solution. Addition of a solution of  $\text{KPF}_6$  (0.28 g; 1.52 mmol) in water (2 ml) caused the separation of a pink solid which was recovered by filtration, washed with water (2 x 2 ml) and dried in vacuo in the presence of  $\text{P}_4\text{O}_{10}$ , affording  $\text{Fe}(\text{L3})_3](\text{PF}_6)_2$  (0.21 g, 94% yield) as a magenta microcrystalline solid. Found (Calcd. for  $\text{C}_{48}\text{H}_{54}\text{F}_{12}\text{FeN}_6\text{P}_2$ ): C: 53.90% (54.35%), H: 4.91% (5.13%), N: 7.85% (7.92%), Fe: 5.08% (5.26%).

$\text{Fe}(\text{L2})_3](\text{PF}_6)_2$ . magenta, from **Fe2-L2** (0.5 mmol). 84% yield. Anal. Found (Calcd. for  $\text{C}_{42}\text{H}_{42}\text{F}_{12}\text{FeN}_6\text{P}_2$ ): C: 51.90% (51.65%), H: 4.1% (4.332%), N: 8.82% (8.60%), Fe: 5.81% (5.72%).

#### 4.4. X-ray structure determinations

Crystal data and collection details for **Fe2-L3**, **Fe2-L4·MeOH** and  $\text{Fe}_6\text{Cl}_6(\mu_4\text{-O})(\mu_2\text{-OMe})_2\{[\text{N,N}-(\text{C}_5\text{H}_5\text{N})\text{C}(\text{CH}_3)\text{N}(2\text{-}^i\text{Pr})\text{C}_6\text{H}_4]\}_2$  are reported in Table X. Data were recorded on a Bruker APEX II diffractometer equipped with a PHOTON100 detector using Mo-K $\alpha$  radiation. Data were corrected for Lorentz polarization and absorption effects (empirical absorption correction SADABS).<sup>25</sup> The structures were solved by direct methods and refined by full-matrix least-squares based on all data using  $F^2$ .<sup>26</sup> Hydrogen atoms were fixed at calculated positions and refined by a riding model. All non-hydrogen atoms were refined with anisotropic displacement parameters.

magari se usi una sigla anche per  $\text{Fe}_6\text{Cl}_6(\mu_4\text{-O})(\mu_2\text{-OMe})_2\{[\text{N},\text{N}-(\text{C}_5\text{H}_5\text{N})\text{C}(\text{CH}_3)\text{N}(2\text{-}^i\text{Pr})\text{C}_6\text{H}_4)]\}_2$  è meglio

**Table 2.** Crystal data and measurement details for **Fe2-L3**, **Fe2-L4-MeOH** and  $\text{Fe}_6\text{Cl}_6(\mu_4\text{-O})(\mu_2\text{-OMe})_2\{[\text{N},\text{N}-(\text{C}_5\text{H}_5\text{N})\text{C}(\text{CH}_3)\text{N}(2\text{-}^i\text{Pr})\text{C}_6\text{H}_4)]\}_2$ .

	<b>Fe2-L3</b>	<b>Fe2-L4-MeOH</b>	$\text{Fe}_6\text{Cl}_6(\mu_4\text{-O})(\mu_2\text{-OMe})_2\{[\text{N},\text{N}-(\text{C}_5\text{H}_5\text{N})\text{C}(\text{CH}_3)\text{N}(2\text{-}^i\text{Pr})\text{C}_6\text{H}_4)]\}_2$
Formula	$\text{C}_{16}\text{H}_{18}\text{Cl}_2\text{FeN}_2$	$\text{C}_{25}\text{H}_{24}\text{Cl}_2\text{FeN}_4\text{O}$	$\text{C}_{40}\text{H}_{60}\text{Cl}_6\text{Fe}_6\text{N}_4\text{O}_{10}$
FW	365.07	523.23	1304.72
T, K	100(2)	100(2)	100(2)
$\lambda$ , Å	0.71073	0.71073	0.71073
Crystal system	Monoclinic	Monoclinic	Monoclinic
Space group	$P2_1/c$	$P2_1/c$	$P2_1/n$
a, Å	11.4318(5)	12.4520(7)	10.8549(10)
b, Å	9.6115(4)	14.8202(8)	11.7831(11)
c, Å	16.1638(7)	13.9596(8)	20.729(2)
$\beta$ , °	108.4800(10)	111.750(2)	100.522(2)
Cell Volume, Å <sup>3</sup>	1684.44(13)	2392.7(2)	2606.7(4)
Z	4	4	2
$D_c$ , g·cm <sup>-3</sup>	1.440	1.452	1.662
$\mu$ , mm <sup>-1</sup>	1.206	0.879	1.988
F(000)	752	1080	1332
Crystal size, mm	0.16×0.13×0.11	0.26×0.22×0.15	0.18×0.16×0.11
$\theta$ limits, °	1.878-28.000	1.761-28.000	1.986-25.999
Reflections collected	25331	35919	33529
Independent reflections	4065 [ $R_{int} = 0.0384$ ]	5782 [ $R_{int} = 0.0291$ ]	5132 [ $R_{int} = 0.0566$ ]
Data/restraints/parameters	4065 / 0 / 193	5782 / 0 / 300	5132 / 0 / 305

Goodness of fit on $F^2$	1.108	1.042	1.209
$R_1$ ( $I > 2\sigma(I)$ )	0.0347	0.0294	0.0611
$wR_2$ (all data)	0.0708	0.0711	0.1243
Largest diff. peak and hole, $e \text{ \AA}^{-3}$	0.424 / -0.368	1.299 / -0.339	0.984 / -0.886

---

**4.5. Polymerization.** Toluene (total volume, 16 ml), isoprene (2 ml, 1,36 g), and MAO were introduced in a 25 ml dried flask in this order. The obtained solution was brought to the desired temperature, and then the iron complex as toluene solution was added. All operations were carried out under dry nitrogen. The polymerization was terminated with methanol containing a small amount of hydrochloric acid; the polymer was coagulated and repeatedly washed with fresh methanol and then dried in vacuum at room temperature.

#### 4.5. Polymer Characterization.

$^{13}\text{C}$  and  $^1\text{H}$  NMR measurements were carried out on a Bruker Avance 400 spectrometer, operating at 400 MHz for  $^1\text{H}$  and 100.58 MHz for  $^{13}\text{C}$ . The spectra were obtained in  $\text{C}_2\text{D}_2\text{Cl}_4$  at  $103^\circ\text{C}$  (hexamethyldisiloxane, HMDS, as internal standard). The concentration of polymer solutions was about 10 wt%.  $^{13}\text{C}$  conditions: 10 mm probe;  $14.50 \mu\text{s}$  as  $90^\circ$  pulse, relaxation delay 18 s; acquisition time 1.87 s. Proton broadband decoupling was achieved with a 1D sequence using `bi_waltz_16_32` power-gated decoupling.

2D experiments.....

DSC scans were carried out on a Perkin-Elmer Pyris 1 instrument equipped with a liquid nitrogen subambient device. The sample, ca. 4 mg, was placed in a sealed aluminum pan, and the measurements were carried out using heating and cooling rates of  $20^\circ\text{C}/\text{min}$ .

The molecular weight averages and the molecular weight distribution (MWD) obtained by Waters GPCV 2000 system using two online detectors: a differential viscosimeter and a refractometer. The experimental conditions consisted of two PLgel Mixed C columns, toluene as mobile phase, 0.8 mL/min flow rate, and  $80^\circ\text{C}$  temperature. The calibration of the GPC system was carried out using 18 narrow MWD polystyrene standards with the molar mass ranging from 162 to  $3.3 \times 10^6$  g/mol.

#### Acknowledgment

## Appendix A. Supplementary material

### References

- 
- <sup>1</sup> G. Ricci, A. Sommazzi, F. Masi, M. Ricci, A. Boglia, G. Leone "Well Defined Transition Metal Complexes with Phosphorus and Nitrogen Ligands for 1,3-Dienes Polymerization" *Coord. Chem. Rev.* **2010**, *254*, 661-676.
- <sup>2</sup> L. Porri, A. Giarrusso, G. Ricci "Recent views on the mechanism of diolefin polymerization with transition metal initiator systems" *Prog. Polym. Sci.* **1991**, *16*, 405-441.
- <sup>3</sup>
- <sup>4</sup>
- <sup>5</sup>
- <sup>6</sup>
- <sup>7</sup>
- <sup>8</sup>
- <sup>9</sup> Y. Zhang, H.J. Zhang, H.M. Ma, Y. WU, *J. Mol. Catal.* **1982**, *17*, 65.
- <sup>10</sup> i) C. Bazzini, A. Giarrusso, L. Porri *Macromol. Rapid Commun.* **2002**, *23*, 9022-927; ii) G. Ricci, D. Morganti, A. Sommazzi, R. Santi, F. Masi *J. Mol. Catal. A: Chemical* **2003**, *204-05*, 287-293;
- <sup>11</sup> i) C. Bazzini, A. Giarrusso, L. Porri, B. Pirozzi, R. Napolitano *Polymer* **2005**, *45*, 2871-2875; ii) B. Pirozzi, R. Napolitano, V. Petraccone, S. Esposito *Macromol. Chem. Phys.* **2004**, *205*, 1343-1350; iii) B. Pirozzi, R. Napolitano, V. Petraccone, S. Esposito *Macromol. Rapid Commun.* **2003**, *24*, 392-396; iv) G. Ricci, F. Bertini, A. C. Boccia, L. Zetta, E. Alberti, B. Pirozzi, A. Giarrusso, L. Porri *Macromolecules* **2007**, *40*, 7238-7243; v) B. Pirozzi, R. Napolitano, G. Giusto, S. Esposito *Macromolecules* **2007**, *40*, 8962-8968.
- <sup>12</sup> Y. Nakayama, Y. Baba; H Yasuda *Macromolecules* **2003**, *36*, 7053-7958.
- <sup>13</sup> J. Raynaud, J. Y. Wu, T. Ritter *Angew. Chem. Int. Ed.* **2012**, *51*, 11805-11808.
- <sup>14</sup> L. Guo, X. Jing, S. Xiong, W. Liu, Z. Liu, C. Chen *Polymers* **2016**, *8*, 389.
- <sup>15</sup> i) Y. Campouret, O. H. Hasmi, M. Visseaux *Coord. Che. Rev.* **2019**, *390*, 127-170; ii) O. H. Hashmi, Y. A. Sommazzi, G. Pampaloni, G. Ricci, F. Masi, G. Leone, Patent Number WO2018073798A1, 2018 (to Versalis S.p.A).
- <sup>16</sup> G. Ricci, G. Leone, A. Boglia, A. C. Boccia, L. Zetta *Macromolecules* **2009**, *42*, 9263-9267.
- <sup>17</sup>



- 
- <sup>18</sup> A. Sommazzi, G. Pampaloni, G. Ricci, F. Masi, G. Leone, Patent Number WO2016042014A1, 2016 (to Versalis S.p.A). G. Pampaloni, G. Ricci, A. Sommazzi, F. Masi, G. Leone, Patent Number WO2017017203A1, 2017 (to Versalis S.p.A). G. Pampaloni, M. Guelfi, A. Sommazzi, G. Leone, F. Masi, S. Zacchini, G. Ricci, *Inorg. Chim. Acta*, **487**, 331-338 (2019).
- <sup>19</sup> (a) J. Raynaud, J. Y. Wu, T. Ritter, *Angew. Chem., Int. Ed.*, **51**, 11805 (2012); (b) T. Ritter, J. Raynaud, J. Y. Wu, Patent N° WO 2012109343 A2 (to President and Fellows of Harvard College), 2012., c) F. Calderazzo, U. Englert, G. Pampaloni, E. Vanni, *C. R. Acad. Sci. Paris, Série II*, **311** (1999); d) L. M. Spencer, R. Altwer, P. Wei, L. Gelmini, J. Gauld, D. W. Stephan, *J. Am. Chem. Soc.*, **22**, 3841 (2003)
- <sup>20</sup> V. C. Gibson, R. K. O'Reilly, D. F. Wass, A. J. P. White, D. J. Williams, *Dalton Trans.*, 2824 (2003). K. Nienkemper, V. V. Kotov, G. Kehr, G. Erker, R. Fröhlich, *Eur. J. Inorg. Chem.*, 366 (2006).
- <sup>21</sup> P.N. Hawker, M. V. Twigg, *Iron(II) and Lower States in Comprehensive Coordination Chemistry*, R.D. Gillard, G. Wilkinson, J.A. McCleverty, Eds., 1987, Vol. 4, pp. 1180-1288; M.V. Twigg, J. Burgess, *Iron in Comprehensive Coordination Chemistry II*, J.A. McCleverty, T.J. Meyer, Eds., 2003, Vol. 5, pp. 405-553
- <sup>22</sup> R. K. Chaggar, J. Fawcett, G.A. Solan, *Acta Cryst.*, **E59**, m462 (2003)
- <sup>23</sup> Some examples are: M. D. Godbole, O. Roubeau, A. M. Mills, H. Kooijman, A. L. Spek, E. Bouwman, *Inorg. Chem.*, **45**, 6713 (2009); A. S. R. Chesman, D. R. Turner, B. Moubaraki, K. S. Murray, G. B. Deacon, S. R. Batten, *Austr. J. Chem.*, **62**, 1137 (2009); K. Mason, I. A. Gass, F. J. White, G. S. Papaefstathiou, E. K. Brechin, P. A. Tasker, *Dalton Trans.*, **40**, 2875 (2011); H. A. Burkill, N. Robertson, R. Vilar, A. J. P. White, J. Williams, *Inorg. Chem.*, **44**, 3337 (2005)
- <sup>24</sup> V. D. Mochel, *J. Polym. Sci. Part A-1: Polym. Chem.* **10** (1972) 1009-1018; H. Sato, Y. Tanaka, *J. Polym. Sci. Part A-1: Polym. Chem.* **17** (1979) 3551-3558.
- <sup>25</sup> G. M. Sheldrick, *SADABS-2008/1 - Bruker AXS Area Detector Scaling and Absorption Correction*, Bruker AXS: Madison, Wisconsin, USA, 2008
- <sup>26</sup> G. M. Sheldrick, *Acta Crystallogr.* **2015**, **71c**, 3-8.